

## Pulse magnetized superconducting bulk array undulator concept

Dian Weerakonda<sup>1,\*</sup>, Anthony Dennis<sup>1</sup>, Marco Calvi<sup>2</sup> and John Durrell<sup>1</sup><sup>1</sup>The Bulk Superconductivity Group, Department of Engineering, University of Cambridge, Cambridge CB2 1PZ, United Kingdom<sup>2</sup>Photon Science Division, Paul Scherrer Institute, Villigen PSI, Switzerland

(Received 29 November 2023; accepted 18 May 2024; published 11 June 2024)

A number of benefits result from reducing the period length of an undulator without sacrificing magnetic field strength, such as an increased photon flux and higher energy synchrotron radiation. Replacing permanent magnets with bulk high-temperature superconductors (HTSs) has proved to be an effective path towards this goal. We present a concept for a bulk HTS undulator that is magnetized via pulsed field magnetization, which is a much more compact and economical form of magnetizing HTS bulks compared to the field-cooling or zero-field cooling methods that are typically employed. The results from an experiment tailored to demonstrate the feasibility of this concept are also presented. With these results, we estimate that an undulator field of 2.3 T could be generated using this design with a magnetic gap of 4 mm and a 16 mm period length, operating at 40 K.

DOI: [10.1103/PhysRevResearch.6.L022060](https://doi.org/10.1103/PhysRevResearch.6.L022060)

A broad range of scientific disciplines make use of synchrotron radiation, generated by a relativistic electron beam passing through an undulator, to probe matter. Typically, the undulating field is produced using rare-earth permanent magnets [1]. Considerable research efforts have focused on reducing the period length of undulators, as this allows higher energy radiation to be generated without having to increase the electron beam energy [2–4]. Furthermore, a short-period undulator allows a higher photon flux to be generated since more undulation periods can fit into the space available [5].

In order to reduce the undulator period length, the size of the permanent magnet pieces must also be reduced, which leads to a reduction in the magnetic field strength. One approach to compensate for this reduction has been to exploit the higher coercivity and remanent fields of rare-earth permanent magnets at lower temperatures by cooling them down to around liquid nitrogen temperatures [6,7]. Low-temperature superconductors (LTSs), such as NbTi or Nb<sub>3</sub>Sn, are an alternative since they allow the generation of very strong magnetic fields. However, the heat load on the superconductor (operating around liquid helium temperatures) due to its close proximity to the electron beam poses a difficult engineering problem [8].

The (RE)Ba<sub>2</sub>Cu<sub>3</sub>O<sub>7-δ</sub> (REBCO) family of high-temperature superconductors (HTSs), where RE is a rare-earth element, has a superconducting transition temperature over 90 K. Therefore, HTSs can operate at much higher temperatures compared to LTSs, where the cooling capacity of cryocoolers is also higher, thus providing a solution to the

heat load problem. Bulk high-temperature superconductors (HTSs) are also capable of trapping very large magnetic fields; a 17.6 T field has been trapped between a stack of two GdBCO bulks at 26 K, each 25 mm in diameter [9]. This has motivated numerous undulator designs incorporating bulk HTSs [8,10–13].

The bulk HTS staggered array design has proved to be a promising route to a high magnetic field and short-period undulator [14,15]. As with all the proposed designs for bulk HTS undulators, this array of bulks needs to be magnetized via field cooling (FC). This typically requires a superconducting solenoid able to fit the bulk undulator array within its bore. An increase in undulator length therefore will often be accompanied by a commensurate increase in the superconducting solenoid length, incurring additional cost.

Here, we present a concept for a bulk HTS undulator that is magnetized via pulsed field magnetization (PFM), which is a much more compact and economical form of magnetizing HTS bulks compared to FC [16]. This is because the pulsed field is generated not using a superconductor, but a normal conductor, such as copper. While PFM often does not lead to trapped fields as high as FC, Zhou *et al.* have reported magnetizing a 36 mm diameter GdBCO disk bulk at 30 K to 4.8 T reliably, which was within 90% of the peak applied field, by exploiting flux jumps [17]. The proposed design also makes use of the full peak field of the bulks, and the height of the bulks can be increased without altering the period length; therefore, this system can potentially reach the same fields as the existing staggered array systems.

Figure 1 illustrates the proposed design for a pulse magnetized bulk HTS undulator. The setup includes two arrays of HTS bulks separated by a few millimetres, the distance required for the electron beam aperture. One side will be offset from the other side horizontally by half of the width of the bulks. This arrangement of the bulks is identical to that proposed by Tanaka *et al.* for a field-cooled bulk array undulator [13]. Additionally, fully independent temperature

\*dw620@cam.ac.uk

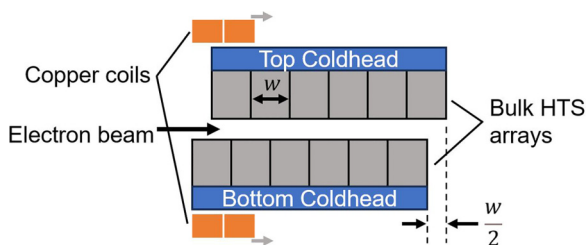


FIG. 1. Schematic illustration of the proposed pulse magnetized bulk HTS undulator. Two arrays of bulks are placed opposite each other with an offset equal to their width ( $w$ ), with independent temperature control for each array. A pair of vortex-type copper coils that can translate from one end to the other is used to generate the pulsed magnetic field.

control must be possible for each array; this can be achieved, as illustrated, by using two separate cryocoolers and temperature control loops for each side. A suitable cryostat (not illustrated) must encase the arrays. The vortex-type copper coils used to generate the pulsed magnetic field will be placed outside the vacuum chamber on either side, in close proximity to the bulks. To improve their efficiency in generating a magnetic field, their electrical resistance should be minimized by cooling them in liquid nitrogen. The magnetic pulse can be generated via the discharge of a bank of capacitors through the coils. The details of such a system can be found in [18].

A cylindrical bulk superconductor carrying current at uniform density everywhere (i.e., in the critical state) will generate a magnetic field on its surface with a central peak and a (approximately) constant gradient, as shown in Fig. 2.

The proposed PFM protocol aims to magnetize every bulk on a single side in the same direction, and the other side will be magnetized in the opposite direction. The sum of the fields from the two arrays will generate an oscillating magnetic field in the electron beam aperture (as shown in Fig. 3).

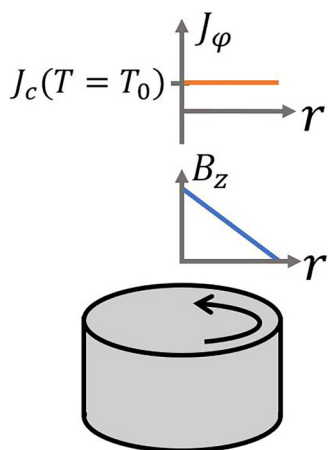


FIG. 2. The current inside and the magnetic field on the surface of a single disk-shaped bulk superconductor in the critical state at a temperature of  $T_0$ .  $J_\phi$  is the current density in the azimuthal direction in the cylindrical coordinate system where the central cylindrical axis of the disk is identical to the  $z$  axis.  $J_c(T)$  is the critical current density at temperature  $T$ .

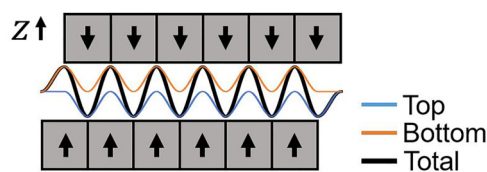


FIG. 3. Magnetization of the bulk array following the proposed PFM protocol. Bulks on one side will be magnetized uniformly in the same direction, with the other side magnetized in the opposite direction. This creates an oscillating magnetic field within the gap between the array.

Zero-field cooling (ZFC) is a technique for magnetizing superconductors where the magnetizing field is applied after the material has been cooled below its critical temperature ( $T_c$ ). PFM is a close analog of ZFC, with the main difference being that ZFC is an isothermal process, while PFM, which leads to rapid magnetic flux penetration in a sample with relatively low thermal diffusivity, is not [19,20]. For clarity, the sequence of pulses required to achieve the bulk magnetization shown in Fig. 3 will be outlined with the assumption that PFM behavior follows ZFC behavior identically. We address the differences that result separately.

Figure 4 shows the suggested PFM protocol. Initially, while the top remains above  $T_c$ , the bottom is cooled to the operating temperature,  $T_0 < T_c$ . Then, a magnetizing pulse in the positive  $z$  direction (indicated in Fig. 3) is applied sequentially to every bulk in the bottom array using the bottom coil. Since the top is above  $T_c$ , it will not be magnetized by the stray field from the bottom coil. Then, the bottom array is cooled to a temperature  $T_L$  that is well below  $T_0$ . Once this cooling process is complete, the top array should be cooled down to  $T_0$ . Now, the top coil can be used to magnetize the top array by applying pulses along its length with the field in the negative  $z$  direction. Now, the top array is fully magnetized in the direction opposite to the bottom array. However, the second round of pulses will induce a small reverse current in the bottom array. The degree to which this reverse current penetrates the surface will be determined by the strength of the stray field from the top coil. But, because the bottom array is well below  $T_0$ , this penetration is minimized. At  $T_L$ , the critical current density ( $J_c$ ) will be increased; therefore, the reverse current that is induced by the stray field will also be of a higher density. Hence, after stage 2 (labeled in Fig. 4) is complete and

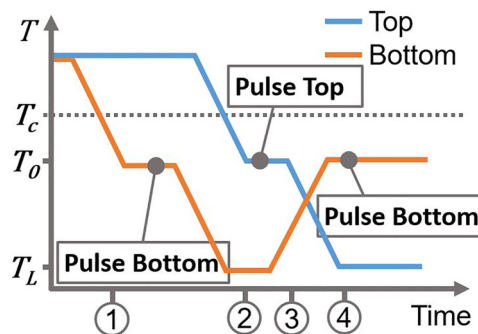


FIG. 4. Proposed PFM protocol to magnetize the bulk undulator array. The circled numbers indicate different stages of the process.

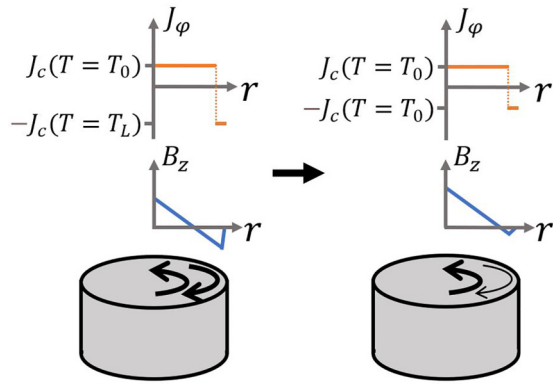


FIG. 5. The change in the current distribution, and hence the magnetic field profile, of a cylindrical bulk superconductor after it is warmed from  $T_L$  to  $T_0$ , where a high reverse current  $J_C(T = T_L)$  is present before warming (left). The reverse current reduces in magnitude until it settles at  $J_C(T = T_0)$  after warming (right).

the temperature of the bottom array is increased from  $T_L$  to  $T_0$ , the bottom array will be unable to maintain the reverse current at  $J_C(T = T_L)$ . This will lead to the reverse current decaying until it settles at the lower value of  $J_C(T = T_0)$ . This process, along with the accompanying trapped field profile change, is illustrated in Fig. 5.

In order to fully remove the reduced yet still present reverse current on the bottom side, another pulse can be applied to every bulk in the bottom array. The field strength of this pulse need not be as high as the pulse which was used to fully magnetize the bottom array during stage 1 because the applied field only needs to penetrate the outer edge of each bulk. Therefore, the stray field from this pulse will have a negligible effect on the magnetization of the top array which has now been cooled to  $T_L$ . Of course, if it is found that the round of weaker pulses to the bottom array still significantly demagnetizes the top, another cycle, of opposite side cooling followed by applying an increasingly weaker pulse, can be repeated until the demagnetization is negligible.

Due to the effectively adiabatic nature of PFM, flux jumps are a common occurrence. A flux jump is a runaway process of magnetic flux migration into the body of a superconductor initiated by a positive feedback loop of temperature increase following flux penetration [21,22]. While this is a highly undesirable phenomenon which magnet engineers carefully avoid when working with conventional wound superconducting magnets, a number of reports exploiting flux jumps to more efficiently magnetize bulk HTSs have been published [20,23,24].

With ZFC, for applied fields which are large enough to penetrate to the center of the bulk, Bean's critical state model [25,26] predicts that the trapped field at the center of a disk-shaped bulk will be linearly proportional to the applied field, provided that it did not exceed the maximum peak field of the bulk. In order to trap the highest possible field within a bulk disk with ZFC, at least twice the maximum possible peak field of the disk needs to be applied. During PFM, however, flux can also penetrate suddenly into the bulk, a process referred to as a flux jump, once a certain threshold

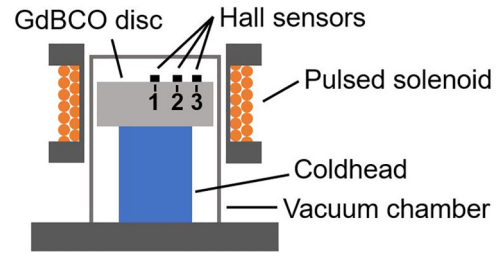


FIG. 6. Experimental setup used to pulse magnetize a GdBCO disk-shaped bulk. A single GdBCO disk, 38 mm in diameter and 12 mm high, is assembled on a coldhead inside a vacuum chamber. A copper solenoid, cooled with LN<sub>2</sub>, placed around the vacuum chamber generated the pulsed field for magnetization. Three Hall sensors (labeled 1–3) placed on the surface of the bulk were used to monitor the trapped field.

pulsed field amplitude is surpassed [23]. Thus, the applied pulse does not necessarily need to be double the maximum possible trapped field in order to trap the highest possible field via PFM. Therefore, if flux jumps are exploited, we can expect the reverse currents induced in the opposite array during the pulsing of one side to be smaller than what would be predicted with the outlined ZFC framework, making the task of their removal easier. Furthermore, this threshold value has been predicted, and experimentally confirmed, to increase with reducing temperature [20]. Therefore, there is no danger of demagnetizing the cooler, already magnetized side from a flux jump.

To validate our assumptions relating to reverse currents induced by negative polarity pulses applied to pre-magnetized HTS bulks, we conducted a simple PFM experiment with a disk-shaped bulk superconductor. As shown in Fig. 6, the GdBCO disk-shaped bulk, 38 mm in diameter and 12 mm high, was assembled on a coldhead cooled by a GM cryocooler. A temperature sensor and a heater were used to control the sample temperature. A copper solenoid, which was cooled with liquid nitrogen (LN<sub>2</sub>) during operation, was placed around the vacuum chamber encasing the sample. This was connected to a bank of capacitors whose discharge, controlled by an IGBT acting as a relay, would produce the pulsed field. Three Hall sensors were placed 1 mm above the surface at  $r = 0$ ,  $r = 7$ , and  $r = 14$  mm, where  $r$  is the distance from the central cylindrical axis of the disk.

Initially, we studied the response of the disk to single pulses of varying amplitude. The sample was heated above  $T_C$  and cooled back down to 70 K for each step. This was used to determine the optimum pulse amplitude which needed to be applied to achieve the highest trapped field. Then, the sample was magnetized with a pulse of this amplitude, cooled to 25 K, and a pulse with the same magnitude but opposite polarity was applied. This simulated the effect of the demagnetization from the stray magnetic field. It should be noted that the stray reverse-direction magnetic field experienced by the opposite array of the proposed undulator is never likely to be equal in magnitude to the initial magnetizing pulse, since the opposite array is always further from the coil. However, this experiment served to test the principle for the worst-case

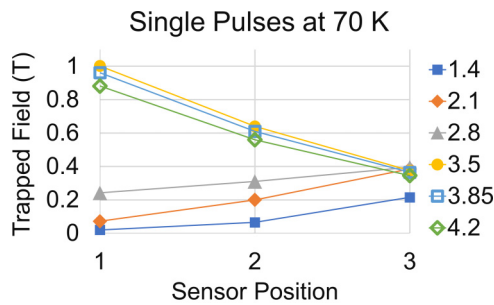


FIG. 7. Single pulse behavior of GdBCO disk bulk at 70 K for varying pulse amplitudes. A peak pulsed field of 3.5 T yields the highest trapped field. Further increases in the applied field lead to a reduction in the trapped field.

scenario. Following the inverted pulse, the sample was heated back up to 70 K and a much weaker positive polarity pulse was applied to remove the reversed edge currents.

The 70 K single pulse profiles at varying pulse amplitudes in Fig. 7 show that a 1.4 T applied field (which refers to the peak amplitude of the pulsed field at the center of the solenoid) is sufficient for the applied field to penetrate to the depth of sensor #2. The maximum trapped field (1.0 T in the center) is achieved with a 3.5 T pulse. Further increases in pulse amplitude lead to a drop in trapped field (a result of the increased heating of the sample at higher applied fields).

The results from each PFM protocol stage are shown in Fig 8. Following the application of a 3.5 T pulse and cooling down to  $T_L$  (25 K), the application of an inverted pulse leads to a reduction in the trapped field at the edge of the sample, as predicted from the ZFC framework utilizing the Bean model. Then, again, as predicted, at the end of stage 3, the increase in temperature from  $T_L$  to  $T_0$  leads to the field at the edges increasing slightly (as the current at the edges decay to the maximum permissible at  $T_0$ ). Finally, at stage 4, the application of a pulse with just over half the amplitude of that which was used during stage 1 fully recovers the lost magnetization from the sample edge. These results demonstrate, therefore, that the demagnetizing effects of the stray field on the opposite array of bulks can be undone.

Using data from [27] for PFM of a disk bulk at 40 K, we estimate that, for our proposed undulator, designed with a 4 mm magnetic gap and a 16 mm period length, an undulator field of 2.3 T could be reached. We have used the formula

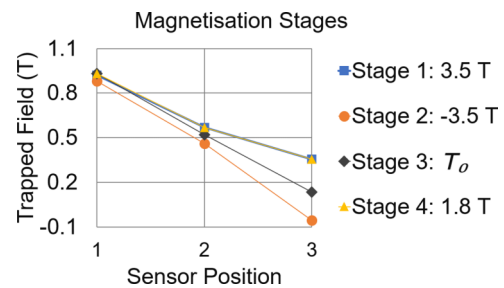


FIG. 8. Trapped field in the bulk during each stage of the magnetization protocol. Stage 1: a 3.5 T field initially magnetizes the disk at 70 K. Stage 2: the disk is cooled to 25 K and pulsed in the reverse direction to simulate the stray field demagnetization. Stage 3: the disk is warmed back up to 70 K. Stage 4: the disk is pulsed with a much weaker pulse to recover the lost magnetization.

for the field above a disk-shaped bulk to compute the effect of increasing the magnetic gap to 4 mm [28]. This field is a factor of 2 higher than what is typically achieved with permanent magnet systems [29]. Repeating the magnetization of the sample in Fig. 6 three times, it was found that the central trapped field changed by up to 1.0% (when the sample temperature was controlled to within 0.05 K between repeats). Therefore, this is an area in which further research is required for improvement.

While there remain several such design aspects in need of optimization, our experiment tailored to verify the feasibility of the proposed pulse magnetized bulk array undulator demonstrates that such a system can indeed be realized. In such a design, a number of benefits over existing bulk HTS undulators are expected, with the cost reduction of the magnetizing fixture being one of the most significant. Furthermore, the undulator field can potentially be tuned and tailored as required by applying multiple pulses to the same section of the array to incrementally increase the trapped field. This could reduce the stringent demands on sample similarity to generate a periodic and sinusoidal-like magnetic field profile along the undulator axis.

The supporting data for this work is openly available on the institutional repository of the University of Cambridge [30].

This work was performed under the auspices and with support from the Swiss Accelerator Research and Technology (CHART) program, and supported by the Engineering & Physical Sciences Research Council (Grant EP/W522120/1) and Oxford Instruments NanoScience.

- [1] J. A. Clarke, *The Science and Technology of Undulators and Wigglers* (Oxford University Press, Oxford, 2004), pp. 111–113.
- [2] H. Kitamura, Recent trends of insertion-device technology for X-ray sources, *J. Synchrotron Radiat.* **7**, 121 (2000).
- [3] T. Schmidt, G. Ingold, A. Imhof, B. Patterson, L. Patthey, C. Quitmann, C. Schulze-Briesse, and R. Abela, Insertion devices

at the Swiss Light Source (phase I), *Nucl. Instrum. Methods Phys. Res. Sect. A* **467–468**, 126 (2001).

- [4] P. M. Stefan, T. Tanabe, S. Krinsky, G. Rakowsky, L. Solomon, and H. Kitamura, Initial results from an in-vacuum undulator in the NSLS X-ray ring, *J. Synchrotron Radiat.* **5**, 417 (1998).
- [5] J.-C. Huang, H. Kitamura, C.-K. Yang, C.-H. Chang, C.-H. Chang, and C.-S. Hwang, Challenges of in-vacuum and

- cryogenic permanent magnet undulator technologies, *Phys. Rev. Accel. Beams* **20**, 064801 (2017).
- [6] T. Hara, T. Tanaka, H. Kitamura, T. Bizen, X. Maréchal, T. Seike, T. Kohda, and Y. Matsuura, Cryogenic permanent magnet undulators, *Phys. Rev. ST Accel. Beams* **7**, 050702 (2004).
- [7] M. Calvi, T. Schmidt, A. Anghel, A. Cervellino, S. J. Leake, P. R. Willmott, and T. Tanaka, Commissioning results of the U14 cryogenic undulator at SLS, *J. Phys.: Conf. Ser.* **425**, 032017 (2013).
- [8] T. Tanaka, T. Hara, R. Tsuru, D. Iwaki, T. Bizen, X. Marechal, T. Seike, and H. Kitamura, Utilization of bulk high-temperature superconductors for shorter-period synchrotron radiation sources, *Supercond. Sci. Technol.* **19**, S438 (2006).
- [9] J. H. Durrell, A. R. Dennis, J. Jaroszynski, M. D. Ainslie, K. G. B. Palmer, Y.-H. Shi, A. M. Campbell, J. Hull, M. Strasik, E. E. Hellstrom, and D. A. Cardwell, A trapped field of 17.6 T in melt-processed, bulk Gd-Ba-Cu-O reinforced with shrink-fit steel, *Supercond. Sci. Technol.* **27**, 082001 (2014).
- [10] M. Calvi, M. D. Ainslie, A. Dennis, J. H. Durrell, S. Hellmann, C. Kittel, D. A. Moseley, T. Schmidt, Y. Shi, and K. Zhang, A GdBCO bulk staggered array undulator, *Supercond. Sci. Technol.* **33**, 014004 (2020).
- [11] R. Kinjo, M. Shibata, T. Kii, H. Zen, K. Masuda, K. Nagasaki, and H. Ohgaki, Demonstration of a high-field short-period undulator using bulk high-temperature superconductor, *Appl. Phys. Express* **6**, 042701 (2013).
- [12] T. Kii, H. Zen, N. Okawachi, M. Nakano, K. Masuda, H. Ohgaki, K. Yoshikawa, and T. Yamazaki, Design study on high-Tc superconducting micro-undulator, in *Proceedings of 28th International Free Electron Laser Conference* (Berlin, 2006), pp. 653–655.
- [13] T. Tanaka, R. Tsuru, and H. Kitamura, Pure-type superconducting permanent-magnet undulator, *J. Synchrotron Radiat.* **12**, 442 (2005).
- [14] M. Calvi, S. Hellmann, E. Prat, T. Schmidt, K. Zhang, A. R. Dennis, J. H. Durrell, and M. D. Ainslie, GdBCO bulk superconducting helical undulator for x-ray free-electron lasers, *Phys. Rev. Res.* **5**, L032020 (2023).
- [15] K. Zhang, A. Pirotta, X. Liang, S. Hellmann, M. Bartkowiak, T. Schmidt, A. Dennis, M. Ainslie, J. Durrell, and M. Calvi, Record field in a 10 mm-period bulk high-temperature superconducting undulator, *Supercond. Sci. Technol.* **36**, 05LT01 (2023).
- [16] J. H. Durrell, M. D. Ainslie, D. Zhou, P. Vanderbemden, T. Bradshaw, S. Speller, M. Filipenko, and D. A. Cardwell, Bulk superconductors: a roadmap to applications, *Supercond. Sci. Technol.* **31**, 103501 (2018).
- [17] D. Zhou, J. Srpcic, K. Huang, M. Ainslie, Y. Shi, A. Dennis, M. Boll, M. Filipenko, D. Cardwell, and J. Durrell, Reliable 4.8 T trapped magnetic fields in Gd-Ba-Cu-O bulk superconductors using pulsed field magnetization, *Supercond. Sci. Technol.* **34**, 034002 (2021).
- [18] Y. K. Tsui, D. Moseley, A. R. Dennis, Y. Shi, M. Beck, V. Ciantanni, D. Cardwell, J. Durrell, and M. Ainslie, Waveform control pulsed field magnetization of RE-Ba-Cu-O bulk superconducting rings, *IEEE Trans. Appl. Supercond.* **32**, 1 (2022).
- [19] M. D. Ainslie, J. Srpcic, D. Zhou, H. Fujishiro, K. Takahashi, D. A. Cardwell, and J. H. Durrell, Toward optimization of multi-pulse, pulsed field magnetization of bulk high-temperature superconductors, *IEEE Trans. Appl. Supercond.* **28**, 1 (2018).
- [20] D. Zhou, M. D. Ainslie, J. Srpcic, K. Huang, Y. Shi, A. R. Dennis, D. A. Cardwell, J. H. Durrell, M. Boll, and M. Filipenko, Exploiting flux jumps for pulsed field magnetisation, *Supercond. Sci. Technol.* **31**, 105005 (2018).
- [21] M. Wilson, *Superconducting Magnets* (Clarendon, Oxford, 1987).
- [22] S. L. Wipf, Review of stability in high temperature superconductors with emphasis on flux jumping, *Cryogenics* **31**, 936 (1991).
- [23] R. Weinstein, D. Parks, R. P. Sawh, K. Carpenter, and K. Davey, A significant advantage for trapped field magnet applications—A failure of the critical state model, *Appl. Phys. Lett.* **107**, 152601 (2015).
- [24] D. Zhou, M. D. Ainslie, Y. Shi, A. R. Dennis, K. Huang, J. R. Hull, D. A. Cardwell, and J. H. Durrell, A portable magnetic field of 3 T generated by the flux jump assisted, pulsed field magnetization of bulk superconductors, *Appl. Phys. Lett.* **110**, 062601 (2017).
- [25] C. P. Bean, Magnetization of hard superconductors, *Phys. Rev. Lett.* **8**, 250 (1962).
- [26] C. P. Bean, Magnetization of high-field superconductors, *Rev. Mod. Phys.* **36**, 31 (1964).
- [27] M. D. Ainslie, H. Fujishiro, H. Mochizuki, K. Takahashi, Y.-H. Shi, D. K. Namburi, J. Zou, D. Zhou, A. R. Dennis, and D. A. Cardwell, Enhanced trapped field performance of bulk high-temperature superconductors using split coil, pulsed field magnetization with an iron yoke, *Supercond. Sci. Technol.* **29**, 074003 (2016).
- [28] I.-G. Chen, J. Liu, R. Weinstein, and K. Lau, Characterization of YBa<sub>2</sub>Cu<sub>3</sub>O<sub>7</sub>, including critical current density  $J_c$ , by trapped magnetic field, *J. Appl. Phys.* **72**, 1013 (1992).
- [29] M. Calvi, C. Camenzuli, R. Ganter, N. Sammut, and T. Schmidt, Magnetic assessment and modelling of the Aramis undulator beamline, *J. Synchrotron Radiat.* **25**, 686 (2018).
- [30] D. Weerakonda, A. Dennis, M. Calvi, and J. Durrell, Research data supporting “Pulse magnetized superconducting bulk array undulator concept”, Apollo - University of Cambridge Repository (2024), doi:10.17863/CAM.108994.